Azimuthally Differential Pion Femtoscopy in Pb-- Pb Collisions at √sNN = 2.76 TeV

(ALICE Collaboration) Adamova, D.; ...; Antičić, Tome; ...; Erhardt, Filip; ...; Gotovac, Sven; ...; Jerčić, Marko; ...; ...

Journal article, Published version
Rad u časopisu, Objavljena verzija rada (izdavačev PDF)

Azimuthally Differential Pion Femtoscopy in Pb-Pb Collisions at $\sqrt{s_{NN}} = 2.76$ TeV

D. Adamová *et al.*[*]

(ALICE Collaboration)

We present the first azimuthally differential measurements of the pion source size relative to the second harmonic event plane in Pb-Pb collisions at a center-of-mass energy per nucleon-nucleon pair of $\sqrt{s_{NN}} = 2.76$ TeV. The measurements have been performed in the centrality range 0%–50% and for pion pair transverse momenta $0.2 < k_T < 0.7$ GeV/c. We find that the R_{side} and R_{out} radii, which characterize the pion source size in the directions perpendicular and parallel to the pion transverse momentum, oscillate out of phase, similar to what was observed at the Relativistic Heavy Ion Collider. The final-state source eccentricity, estimated via R_{side} oscillations, is found to be significantly smaller than the initial-state source eccentricity, but remains positive—indicating that even after a stronger expansion in the in-plane direction, the pion source at the freeze-out is still elongated in the out-of-plane direction. The $3 + 1$D hydrodynamic calculations are in qualitative agreement with observed centrality and transverse momentum R_{side} oscillations, but systematically underestimate the oscillation magnitude.

It was first shown in 1960 that the distribution of pions emitted in $p\bar{p}$ collisions at small relative angles is affected by quantum statistical effects and is sensitive to the size of the emitting source [1]. Since then, the correlation technique with two identical particles at small relative momentum, often called intensity, or Hanbury Brown-Twiss (HBT) interferometry [2–6], has been used to study the space-time structure of the pion-emitting source from hadron-hadron and electron-positron to heavy-ion collisions (for a review, see Ref. [7]). The so-called HBT radii, obtained in these analyses, characterize the spatial and temporal extent of the source emitting pions of a given momentum, the extensions of the so-called homogeneity regions. Because of the position-momentum correlations in particle emission, the HBT radii become sensitive to the collective velocity fields, and as such provide information on the dynamics of the system evolution [7]. Recent measurements of the centrality dependence of the HBT radii in Pb-Pb collisions at LHC energies [8] further confirm the scaling of the effective source volume with the particle rapidity density as well as stronger radial flow at higher energies.

Pion interferometry of anisotropic sources (azimuthally differential femtoscopy) was suggested in Refs. [9,10], and the corresponding measurements [11] appeared shortly after strong directed and in-plane elliptic flow were measured in Au-Au collisions at the Alternating Gradient Synchrotron (AGS) [12,13]. Anisotropic flow, the response

of the system to the initial geometry, is usually characterized by the Fourier decomposition of the particle azimuthal distribution and quantified by the harmonic strength and orientation of the corresponding flow plane. Azimuthally differential femtoscopic measurements can be performed relative to different harmonic flow planes, providing important complementary information on the particle source. For example, the measurements of HBT radii with respect to the first harmonic (directed) flow at the AGS [14] revealed that the source was tilted relative to the beam direction [15]. Azimuthal dependence of the HBT radii relative to the higher harmonic ($n > 2$) flow planes can originate only from the anisotropies in collective flow gradients [16,17] and the observation [18] of such a modulation unambiguously signals a collective expansion and anisotropy in the flow fields. In particular, measurements of HBT radii with respect to the second harmonic (elliptic) flow provide information on the evolution of the system shape, which is expected to become more spherical at freeze-out compared to the initial state due to stronger in-plane expansion. In the recent RHIC beam energy scan, it was found that the eccentricity at freeze-out decreases continuously with increasing beam energy [19], a trend consistent with predictions by hydrodynamic and hadronic transport models [20,21]. Earlier measurements [22,23] showed that even at the highest RHIC energies the source at freeze-out remains out-of-plane extended, albeit with eccentricities significantly lower than the initial ones. Hydrodynamical calculations [20] predicted that at the Large Hadron Collider (LHC) energies, about an order of magnitude higher than the top RHIC energy, the pion source should eventually become isotropic, or even in-plane extended.

In this Letter, we present the first azimuthally differential femtoscopic measurements relative to the second harmonic

---

[*]Full author list given at the end of the article.

flow plane in Pb-Pb collisions at $\sqrt{s_{NN}} = 2.76$ TeV from the ALICE experiment at the CERN-LHC and compare the results to previous measurements at RHIC energies and to model calculations.

The data were recorded in 2011 during the second Pb-Pb running period of the LHC. Approximately 2 million minimum bias events, 29.2 million central trigger events, and 34.1 million semicentral trigger events were used in this analysis. A detailed description of the ALICE detector can be found in Refs. [24,25]. The Time Projection Chamber (TPC) has full azimuthal coverage and allows charged-particle track reconstruction in the pseudorapidity range $|\eta| < 0.8$, as well as particle identification via the specific ionization energy loss dE/dx associated with each track. In addition to the TPC, the time-of-flight (TOF) detector was used for identification of particles with transverse momentum $p_T > 0.5$ GeV/c.

The minimum bias, semicentral, and central triggers used in this analysis all require a signal in both V0 detectors [26]. The V0 is a small angle detector of scintillator arrays covering pseudorapidity ranges $2.8 < \eta < 5.1$ and $-3.7 < \eta < -1.7$ for a collision vertex occurring at the center of the ALICE detector. The V0 detector was also used for the centrality determination [8]. The results of this analysis are reported for collision centrality classes expressed as ranges of the fraction of the inelastic Pb-Pb cross section: 0%–5%, 5%–10%, 10%–20%, 20%–30%, 30%–40%, and 40%–50%. The position of the primary event vertex along the beam direction V_z was determined for each event. Events with $|V_z| < 8$ cm were used in this analysis to ensure a uniform pseudorapidity acceptance.

The TPC has 18 sectors covering the full azimuth with 159 pad rows radially placed in each sector. Tracks with at least 80 space points in the TPC have been used in this analysis. Tracks compatible with a decay in flight (kink topology) were rejected. The track quality was determined by the χ^2 of the Kalman filter fit to the reconstructed TPC clusters. The χ^2 per degrees of freedom was required to be less than 4. For primary track selection, only trajectories passing within 3.2 cm from the primary vertex in the longitudinal direction and 2.4 cm in the transverse direction were used. Based on the specific ionization energy loss in the TPC gas compared with the corresponding Bethe-Bloch curve, and the time of flight in the TOF detector, a probability for each track to be a pion, kaon, proton, or electron was determined. Particles for which the pion probability was the largest were used in this analysis. Pions were selected in the pseudorapidity range $|\eta| < 0.8$ and $0.15 < p_T < 1.5$ GeV/c.

The correlation function $C(\mathbf{q})$ was calculated as

$$C(\mathbf{q}) = \frac{A(\mathbf{q})}{B(\mathbf{q})}, \qquad (1)$$

where $\mathbf{q} = \mathbf{p}_1 - \mathbf{p}_2$ is the relative momentum of two pions, $A(\mathbf{q})$ is the same-event distribution of particle pairs, and

$B(\mathbf{q})$ is the background distribution of uncorrelated particle pairs. Both the $A(\mathbf{q})$ and $B(\mathbf{q})$ distributions were measured differentially with respect to the second harmonic event-plane angle $\Psi_{EP,2}$. The second harmonic event-plane angle $\Psi_{EP,2}$ was determined using TPC tracks. To avoid self-correlation, each event was split into two subevents ($-0.8 < \eta < 0$ and $0 < \eta < 0.8$). Pairs were chosen from one subevent and the second harmonic event-plane angle $\Psi_{EP,2}$ was determined using the other subevent particles, and vice versa, with the event plane resolution determined from the correlations between the event planes determined in different subevents [27]. The background distribution is built by using the mixed-event technique [4] in which pairs are made out of particles from two different events with similar centrality (less than 2% difference), event-plane angle (less than 10° difference), and event vertex position along the beam direction (less than 4 cm difference). Requiring a minimum value in the two-track separation parameters $\Delta\varphi^*$ and $\Delta\eta$ controls two-track reconstruction effects such as track splitting or track merging. The quantity φ^* is defined in this analysis as the azimuthal angle of the track in the laboratory frame at the radial position of 1.6 m inside the TPC. Splitting is the effect when one track is reconstructed as two tracks, and merging is the effect of two tracks being reconstructed as one. Also, to reduce the splitting effect, pairs that share more than 5% of the TPC clusters were removed from the analysis. It is observed that at large relative momentum the correlation function is a constant, and the background pair distribution is normalized such that this constant is unity. The analysis was performed for different collision centralities in several ranges of k_T, the magnitude of the pion-pair transverse momentum $\mathbf{k}_T = (\mathbf{p}_{T,1} + \mathbf{p}_{T,2})/2$, and in bins of $\Delta\varphi = \varphi_{\text{pair}} - \Psi_{EP,2}$, defined in the range $(0, \pi)$ where φ_{pair} is the pair azimuthal angle. The Bertsch-Pratt [5,6] out-side-long coordinate system was used with the *long* direction pointing along the beam axis, *out* along the transverse pair momentum, and *side* being perpendicular to the other two. The three-dimensional correlation function was analyzed in the Longitudinally Co-Moving System (LCMS), in which the total longitudinal momentum of the pair is zero, $p_{1,L} = -p_{2,L}$.

To isolate the Bose-Einstein contribution in the correlation function, effects due to final-state Coulomb repulsion must be taken into account. For that, the Bowler-Sinyukov fitting procedure [28,29] was used in which the Coulomb weight is only applied to the fraction of pairs (λ) that participate in the Bose-Einstein correlation. In this approach, the correlation function is fitted to

$$C(\mathbf{q}, \Delta\varphi) = N\{(1-\lambda) + \lambda K(\mathbf{q})[1 + G(\mathbf{q}, \Delta\varphi)]\}, \quad (2)$$

where N is the normalization factor. The function $G(\mathbf{q}, \Delta\varphi)$ describes the Bose-Einstein correlations and $K(\mathbf{q})$ is the Coulomb part of the two-pion wave function integrated

over a source function corresponding to $G(\mathbf{q})$. In this analysis, the Gaussian form of $G(\mathbf{q}, \Delta\varphi)$ was used [30]:

$$G(\mathbf{q}, \Delta\varphi) = \exp\left[-q_{\text{out}}^2 R_{\text{out}}^2(\Delta\varphi) - q_{\text{side}}^2 R_{\text{side}}^2(\Delta\varphi)\right.$$
$$- q_{\text{long}}^2 R_{\text{long}}^2(\Delta\varphi) - 2q_{\text{out}}q_{\text{side}}R_{\text{os}}^2(\Delta\varphi)$$
$$\left. - 2q_{\text{side}}q_{\text{long}}R_{\text{sl}}^2(\Delta\varphi) - 2q_{\text{out}}q_{\text{long}}R_{\text{ol}}^2(\Delta\varphi)\right],$$
$$(3)$$

where the parameters R_{out}, R_{side}, and R_{long} are traditionally called HBT radii in the *out*, *side*, and *long* directions. The cross terms R_{os}^2, R_{sl}^2, and R_{ol}^2 describe the correlation in the *out- side*, *side- long*, and *out- long* directions, respectively.

The systematic errors on the extracted radii vary within 3%–9% depending on k_T and centrality. They include uncertainties related to the tracking efficiency and track quality, momentum resolution [31], different pair cuts ($\Delta\varphi^*$ and $\Delta\eta$), and correlation function fit ranges. Positive and negative pion pairs, as well as data obtained with two opposite magnetic field polarities of the ALICE L3 magnet, have been analyzed separately and a small difference in the results (less than 3%) has been also accounted for in the systematic error. The total systematic errors were obtained from adding the above systematic errors in quadrature.

Other than being differential in the event plane, this analysis is similar in most aspects to the analysis reported in [31], and further details can be found there. The results reported below were obtained with the second harmonic event plane [27] determined with the TPC tracks. It was checked that they are consistent with the results obtained with the event-plane angle determined with the V0 detector.

Figure 1 presents the dependence of R_{out}^2, R_{side}^2, R_{long}^2, R_{os}^2, and λ on the pion emission angle relative to the second harmonic event plane. The results are shown for the centrality classes 20%–30% in four ranges of k_T: 0.2–0.3, 0.3–0.4, 0.4–0.5, and 0.5–0.7 GeV/c. R_{out}^2 and R_{side}^2 exhibit clear out-of-phase oscillations. No oscillations for R_{long}^2 and λ are observed within the uncertainties of the measurement. The parameter R_{os}^2 shows very similar oscillations for all k_T bins. R_{ol}^2 and R_{sl}^2 (not shown) are found to be consistent with zero, as expected due to symmetry, and are not further investigated in this analysis. A possible correlation between λ and the extracted radii was checked by fixing λ. No change in the radii has been observed. The curves represent the fits to the data using the functions [9,10]

$$R_{\mu}^2(\Delta\varphi) = R_{\mu,0}^2 + 2R_{\mu,2}^2 \cos(2\Delta\varphi) (\mu = \text{out}, \text{side}, \text{long}, \text{sl}, \text{ol}),$$
$$R_{\text{os}}^2(\Delta\varphi) = R_{\text{os},0}^2 + 2R_{\text{os},2}^2 \sin(2\Delta\varphi). \qquad (4)$$

Fitting the radii's azimuthal dependence with the functional form of Eq. (4) allows us to extract the average radii and the amplitudes of oscillations. The latter have to be corrected for the finite event plane resolution. There exist several methods
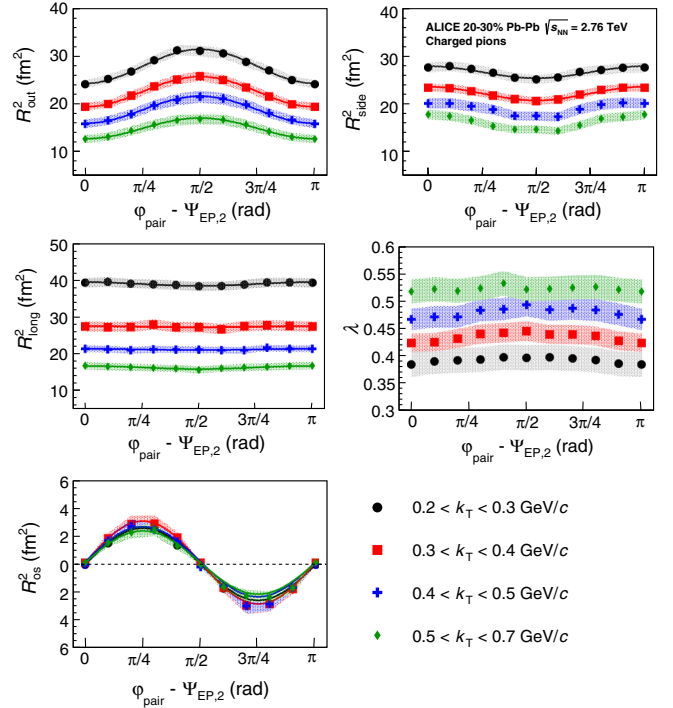

FIG. 1.   The azimuthal dependence of R_{out}^2, R_{side}^2, R_{long}^2, R_{os}^2, and λ as a function of $\Delta\varphi = \varphi_{\text{pair}} - \Psi_{\text{EP},2}$ for the centrality 20%–30% and k_T ranges 0.2–0.3, 0.3–0.4, 0.4–0.5, and 0.5–0.7 GeV/c. Bands indicate the systematic errors. The results are not corrected for the event plane resolution of about 85%–95%.

for such a correction [7], which produce very similar results [19] well within errors of this analysis. The results shown below have been obtained with the simplest method first used by the E895 Collaboration [14], in which the amplitude of oscillation is divided by the event plane resolution factor. The correction is about 5%–15%, depending on centrality. Figure 2 shows the average radii for different k_T values as a function of centrality. The average radii obtained in this analysis are consistent with the results reported in Ref. [31]. As expected, the radii are larger in more central collisions and at smaller k_T values, the latter reflecting the effect of radial flow [7,32]. The cross term $R_{\text{os},0}^2$ is consistent with zero, as expected due to the symmetry of the system. Figure 2 also shows the average radii calculated for charged pions in the pseudorapidity range $|\eta| < 2$ from $3 + 1$D hydrodynamic calculations [33], assuming freeze-out temperature $T_f = 150$ MeV and a constant shear viscosity to entropy density ratio $\eta/s = 0.08$. The $3 + 1$D hydrodynamic calculations, while correctly describing the qualitative features of the average radii dependence on centrality and k_T, fail to describe our results quantitatively.

Figure 3 shows the relative amplitudes of the radius oscillations $R_{\text{out},2}^2/R_{\text{side},0}^2$, $R_{\text{side},2}^2/R_{\text{side},0}^2$, $R_{\text{long},2}^2/R_{\text{long},0}^2$, and $R_{\text{os},2}^2/R_{\text{side},0}^2$. When comparing our results to the ones obtained by the STAR experiment, we observe similar relative oscillations; however, STAR results [22,23] show
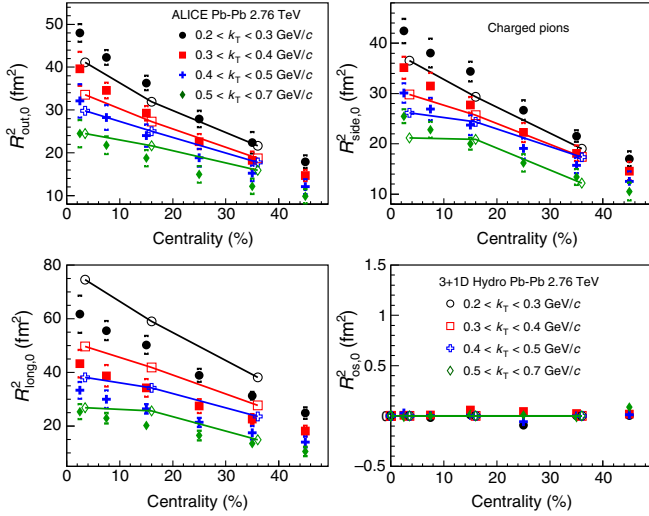
FIG. 2. The average radii $R^2_{out,0}$, $R^2_{side,0}$, $R^2_{long,0}$, and $R^2_{os,0}$ as a function of centrality for different k_T ranges compared to hydrodynamical calculations [33]. Square brackets indicate the systematic errors.

on average larger oscillations for R^2_{side}. Our relative amplitudes for $R^2_{out,2}/R^2_{side,0}$, $R^2_{side,2}/R^2_{side,0}$, and $R^2_{os,2}/R^2_{side,0}$ show a clear centrality dependence, whereas the $R^2_{long,2}/R^2_{long,0}$ is very close to zero for all centralities, similarly to the results from RHIC [19,22,34].

The source eccentricity is usually defined as $\varepsilon = (R^2_y - R^2_x)/(R^2_y + R^2_x)$, where R_x is the in-plane radius of the (assumed) elliptical source and R_y is the out-of-plane
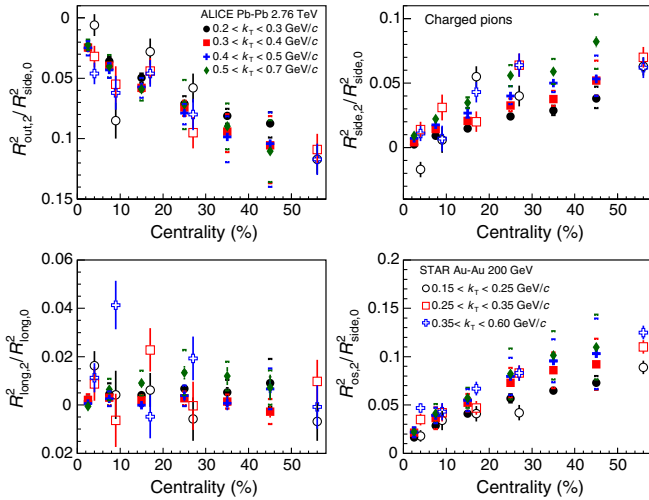

FIG. 3. Amplitudes of the relative radius oscillations $R^2_{out,2}/R^2_{side,0}$, $R^2_{side,2}/R^2_{side,0}$, $R^2_{long,2}/R^2_{long,0}$, and $R^2_{os,2}/R^2_{side,0}$ versus centrality for the k_T ranges 0.2–0.3, 0.3–0.4, 0.4–0.5, and 0.5–0.7 GeV/c. The error bars indicate the statistical uncertainties and the square brackets show the systematic errors. The STAR data points, for 0%–5%, 5%–10%, 10%–20%, 20%–30% and 30%–80% Au-Au collisions, are slightly shifted for clarity.

radius. As shown in Ref. [32] the relative amplitudes of side radii oscillations are mostly determined by the spatial source anisotropy and are less affected by dynamical effects such as velocity gradients. The source eccentricity at freeze-out ε_{final} can be estimated from R^2_{side} oscillations at small pion momenta with an accuracy within 20%–30% as $\varepsilon_{final} \approx 2R^2_{side,2}/R^2_{side,0}$ [32].

Figure 4 presents $2R^2_{side,2}/R^2_{side,0}$ for different k_T ranges as a function of the initial-state eccentricity for six different centralities and four k_T bins. For the initial eccentricity, we have used the nucleon participant eccentricity from the Monte Carlo Glauber model for both, Au-Au collisions at $\sqrt{s_{NN}} = 200$ GeV [18] and Pb-Pb collision at $\sqrt{s_{NN}} = 2.76$ TeV [35]. Our results for all k_T bins are significantly below the values of the initial eccentricity indicating a more intense expansion in the in-plane direction. Due to relatively large uncertainties of the RHIC results for narrow k_T bins, we compare our results only to the average STAR data [22] in $0.15 < k_T < 0.6$ GeV/c and to PHENIX results [18] corresponding to $0.2 < k_T < 2.0$ GeV/c ($\langle k_T \rangle = 0.53$ GeV/c). We find a smaller final-state anisotropy in the LHC regime compared to RHIC energies. This trend is qualitatively consistent with expectations from hydrodynamic and transport models [20,21]. The final-state eccentricity remains positive also at the LHC, evidence of an out-of-plane elongated source at freeze-out. In Fig. 4, we also compare our results to the $3 + 1$D hydrodynamic calculations [33], which were performed for similar centralities and k_T ranges as in the experiment. This model slightly underestimates the final source eccentricity.

In conclusion, we have performed a measurement of two-pion azimuthally differential femtoscopy relative to the second harmonic flow plane in Pb-Pb collisions at $\sqrt{s_{NN}} = 2.76$ TeV. The out, side, and out-side radii exhibit clear oscillations while the long radius is consistent with a
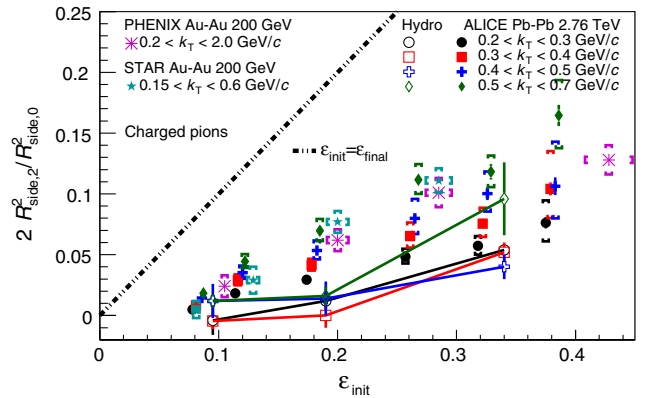

FIG. 4. An estimate of freeze-out eccentricity $2R^2_{side,2}/R^2_{side,0}$ for different k_T ranges vs initial state eccentricity from the Monte Carlo Glauber model [35] for six centrality ranges, 0%–5%, 5%–10%, 10%–20%, 20%–30%, 30%–40%, and 40%–50%. The dashed line indicates $\varepsilon_{final} = \varepsilon_{init}$. Square brackets indicate systematic errors.

constant. The relative amplitudes of oscillations only weakly depend on k_T, with the side-radii oscillation slightly increasing with k_T. The final-state source eccentricity, estimated via side-radius oscillations, is noticeably smaller than at lower collisions energies, but still exhibits an out-of-plane elongated source at freeze-out even after a stronger in-plane expansion. The final eccentricity is slightly larger than that predicted by existing hydrodynamic calculations.

[1] G. Goldhaber, S. Goldhaber, W. Lee, and A. Pais, Influence of Bose-Einstein statistics on the anti-proton proton annihilation process, Phys. Rev. **120**, 300 (1960).

[2] G. I. Kopylov and M. I. Podgoretsky, Correlations of identical particles emitted by highly excited nuclei, Sov. J. Nucl. Phys. **15**, 219 (1972).

[3] G. I. Kopylov and M. I. Podgoretsky, Multiple production and interference of particles emitted by moving sources, Sov. J. Nucl. Phys. **18**, 336 (1974).

[4] G. Kopylov, Like particle correlations as a tool to study the multiple production mechanism, Phys. Lett. **B50**, 472 (1974).

[5] S. Pratt, Pion interferometry of Quark-Gluon Plasma, Phys. Rev. D **33**, 1314 (1986).

[6] G. Bertsch, M. Gong, and M. Tohyama, Pion interferometry in ultrarelativistic heavy-ion collisions, Phys. Rev. C **37**, 1896 (1988).

[7] M. A. Lisa, S. Pratt, R. Soltz, and U. Wiedemann, Femtoscopy in relativistic heavy ion collisions, Annu. Rev. Nucl. Part. Sci. **55**, 357 (2005).

[8] K. Aamodt *et al.* (ALICE Collaboration), Centrality Dependence of the Charged-Particle Multiplicity Density at Mid-Rapidity in Pb-Pb Collisions at $\sqrt{s_{NN}} = 2.76$ TeV, Phys. Rev. Lett. **106**, 032301 (2011).

[9] S. A. Voloshin and W. E. Cleland, HBT analysis of anisotropic transverse flow, Phys. Rev. C **53**, 896 (1996).

[10] S. A. Voloshin and W. E. Cleland, Anisotropic transverse flow and the HBT correlation function, Phys. Rev. C **54**, 3212 (1996).

[11] D. Miskowiec (E877 Collaboration), Pion-pion correlations in Au + Au collisions at AGS energy, Nucl. Phys. **A590**, 473 (1995).

[12] J. Barrette *et al.* (E877 Collaboration), Observation of Anisotropic Event Shapes and Transverse Flow in Au + Au Collisions at AGS Energy, Phys. Rev. Lett. **73**, 2532 (1994).

[13] J. Barrette *et al.* (E877 Collaboration), Energy and charged particle flow in a 10.8A GeV/c Au + Au collisions, Phys. Rev. C **55**, 1420 (1997).

[14] M. A. Lisa (E895 Collaboration) *et al.*, Azimuthal dependence of pion interferometry at the AGS, Phys. Lett. **B496**, 1 (2000).

[15] M. A. Lisa, U. W. Heinz, and U. A. Wiedemann, Tilted pion sources from azimuthally sensitive HBT interferometry, Phys. Lett. **B489**, 287 (2000),

[16] S. A. Voloshin, Femtoscopy of the system shape fluctuations in heavy ion collisions, J. Phys. G **38**, 124097 (2011).

[17] C. J. Plumberg, C. Shen, and U. W. Heinz, Hanbury Brown-Twiss interferometry relative to the triangular flow plane in heavy-ion collisions, Phys. Rev. C **88**, 044914 (2013).

[18] , A. Adare *et al.* (PHENIX Collaboration), Azimuthal-Angle Dependence of Charged-Pion-Interferometry Measurements with Respect to Second- and Third-Order Event Planes in Au + Au Collisions at $\sqrt{s_{NN}} = 200$ GeV, Phys. Rev. Lett. **112**, 222301 (2014).

[19] L. Adamczyk *et al.* (STAR Collaboration), Beam-energy-dependent two-pion interferometry and the freeze-out eccentricity of pions measured in heavy ion collisions at the STAR detector, Phys. Rev. C **92**, 01494 (2015).

[20] C. Shen and U. Heinz, Viscous Flow in Heavy-Ion Collisions from RHIC to LHC, Nucl. Phys. **A904–905**, 361c (2013).

[21] M. A. Lisa, E. Frodermann, G. Graef, M. Mitrovski, E. Mount, H. Petersen, and M. Bleicher, Shape analysis of strongly-interacting systems: the heavy ion case, New J. Phys. **13**, 065006 (2011).

[22] J. Adams *et al.* (STAR Collaboration), Azimuthally Sensitive HBT in Au + Au Collisions at $\sqrt{s_{NN}} = 200$ GeV, Phys. Rev. Lett. **93**, 012301 (2004).

[23] J. Adams *et al.* (STAR Collaboration), Pion interferometry in Au + Au collisions at $\sqrt{s_{NN}} = 200$ GeV, Phys. Rev. C **71**, 044906 (2005).

[24] K. Aamodt *et al.* (ALICE Collaboration), The ALICE experiment at the CERN LHC, J. Instrum. **3**, S08002 (2008).

[25] B. Abelev *et al.* (ALICE Collaboration), Performance of the ALICE Experiment at the CERN LHC, Int. J. Mod. Phys. A **29**, 1430044 (2014).

[26] E. Abbas *et al.* (ALICE Collaboration), Performance of the ALICE VZERO system, J. Instrum. **8**, P10016 (2013).

[27] A. M. Poskanzer and S. A. Voloshin, Methods for analyzing anisotropic flow in relativistic nuclear collisions, Phys. Rev. C **58**, 1671 (1998).

[28] M. G. Bowler, Bose-Einstein correlations in quark initiated jets, Part. World **2**, 1 (1991).

[29] Y. Sinyukov, R. Lednicky, S. Akkelin, J. Pluta, and B. Erazmus, Coulomb corrections for interferometry analysis of expanding hadron systems, Phys. Lett. B **432**, 248 (1998).

[30] S. Pratt, T. Csörgő, and J. Zimányi, Detailed predictions for two-pion correlations in ultrarelativistic heavy-ion collisions, Phys. Rev. C **42**, 2646 (1990).

[31] J. Adam *et al.* (Alice Collaboration), Centrality dependence of pion freeze-out radii in Pb-Pb collisions at $\sqrt{s_{NN}} = 2.76$ TeV, Phys. Rev. C **93**, 024905 (2016).

[32] F. Retiere and M. A. Lisa, Observable implications of geometrical and dynamical aspects of freeze out in heavy ion collisions, Phys. Rev. C **70**, 044907 (2004).

[33] P. Bozek, Azimuthally sensitive femtoscopy in event-by-event hydrodynamics, Phys. Rev. C **89**, 044904 (2014).

[34] A. Adare *et al.* (PHENIX Collaboration), Systematic study of charged-pion and kaon femtoscopy in Au + Au collisions at $\sqrt{s_{NN}} = 200$ GeV, Phys. Rev. C **92**, 034914 (2015).

[35] S. Ghosh, S. K. Singh, S. Chatterjee, J. Alam, and S. Sarkar, Initial conditions from the shadowed Glauber model for Pb + Pb collisions at $\sqrt{s_{NN}} = 2.76$ TeV, Phys. Rev. C **93**, 054904 (2016).

D. Adamová,[87] M. M. Aggarwal,[91] G. Aglieri Rinella,[34] M. Agnello,[30,113] N. Agrawal,[47] Z. Ahammed,[139] S. Ahmad,[17] S. U. Ahn,[69] S. Aiola,[143] A. Akindinov,[54] S. N. Alam,[139] D. S. D. Albuquerque,[124] D. Aleksandrov,[83] B. Alessandro,[113] D. Alexandre,[104] R. Alfaro Molina,[64] A. Alici,[12,107] A. Alkin,[3] J. Alme,[21,36] T. Alt,[41] S. Altinpinar,[21] I. Altsybeev,[138] C. Alves Garcia Prado,[123] M. An,[7] C. Andrei,[80] H. A. Andrews,[104] A. Andronic,[100] V. Anguelov,[96] C. Anson,[90] T. Antičić,[101] F. Antinori,[110] P. Antonioli,[107] R. Anwar,[126] L. Aphecetche,[116] H. Appelshäuser,[60] S. Arcelli,[26] R. Arnaldi,[113] O. W. Arnold,[97,35] I. C. Arsene,[20] M. Arslandok,[60] B. Audurier,[116] A. Augustinus,[34] R. Averbeck,[100] M. D. Azmi,[17] A. Badalà,[109] Y. W. Baek,[68] S. Bagnasco,[113] R. Bailhache,[60] R. Bala,[93] A. Baldisseri,[65] M. Ball,[44] R. C. Baral,[57]

A. M. Barbano,[25] R. Barbera,[27] F. Barile,[32] L. Barioglio,[25] G. G. Barnaföldi,[142] L. S. Barnby,[104,34] V. Barret,[71] P. Bartalini,[7] K. Barth,[34] J. Bartke,[120,†] E. Bartsch,[60] M. Basile,[26] N. Bastid,[71] S. Basu,[139] B. Bathen,[61] G. Batigne,[116] A. Batista Camejo,[71] B. Batyunya,[67] P. C. Batzing,[20] I. G. Bearden,[84] H. Beck,[96] C. Bedda,[30] N. K. Behera,[50] I. Belikov,[135] F. Bellini,[26] H. Bello Martinez,[2] R. Bellwied,[126] L. G. E. Beltran,[122] V. Belyaev,[76] G. Bencedi,[142] S. Beole,[25] A. Bercuci,[80] Y. Berdnikov,[89] D. Berenyi,[142] R. A. Bertens,[53,129] D. Berzano,[34] L. Betev,[34] A. Bhasin,[93] I. R. Bhat,[93] A. K. Bhati,[91] B. Bhattacharjee,[43] J. Bhom,[120] L. Bianchi,[126] N. Bianchi,[73] C. Bianchin,[141] J. Bielčík,[38] J. Bielčíková,[87] A. Bilandzic,[35,97] G. Biro,[142] R. Biswas,[4] S. Biswas,[4] J. T. Blair,[121] D. Blau,[83] C. Blume,[60] G. Boca,[136] F. Bock,[75,96] A. Bogdanov,[76] L. Boldizsár,[142] M. Bombara,[39] G. Bonomi,[137] M. Bonora,[34] J. Book,[60] H. Borel,[65] A. Borissov,[99] M. Borri,[128] E. Botta,[25] C. Bourjau,[84] P. Braun-Munzinger,[100] M. Bregant,[123] T. A. Broker,[60] T. A. Browning,[98] M. Broz,[38] E. J. Brucken,[45] E. Bruna,[113] G. E. Bruno,[32] D. Budnikov,[102] H. Buesching,[60] S. Bufalino,[30,25] P. Buhler,[115] S. A. I. Buitron,[62] P. Buncic,[34] O. Busch,[132] Z. Buthelezi,[66] J. B. Butt,[15] J. T. Buxton,[18] J. Cabala,[118] D. Caffarri,[34] H. Caines,[143] A. Caliva,[53] E. Calvo Villar,[105] P. Camerini,[24] A. A. Capon,[115] F. Carena,[34] W. Carena,[34] F. Carnesecchi,[26,12] J. Castillo Castellanos,[65] A. J. Castro,[129] E. A. R. Casula,[23,108] C. Ceballos Sanchez,[9] P. Cerello,[113] B. Chang,[127] S. Chapeland,[34] M. Chartier,[128] J. L. Charvet,[65] S. Chattopadhyay,[139] S. Chattopadhyay,[103] A. Chauvin,[97,35] M. Cherney,[90] C. Cheshkov,[134] B. Cheynis,[134] V. Chibante Barroso,[34] D. D. Chinellato,[124] S. Cho,[50] P. Chochula,[34] K. Choi,[99] M. Chojnacki,[84] S. Choudhury,[139] P. Christakoglou,[85] C. H. Christensen,[84] P. Christiansen,[33] T. Chujo,[132] S. U. Chung,[99] C. Cicalo,[108] L. Cifarelli,[12,26] F. Cindolo,[107] J. Cleymans,[92] F. Colamaria,[32] D. Colella,[55,34] A. Collu,[75] M. Colocci,[26] G. Conesa Balbastre,[72] Z. Conesa del Valle,[51] M. E. Connors,[143,‡] J. G. Contreras,[38] T. M. Cormier,[88] Y. Corrales Morales,[113] I. Cortés Maldonado,[2] P. Cortese,[31] M. R. Cosentino,[125] F. Costa,[34] S. Costanza,[136] J. Crkovská,[51] P. Crochet,[71] E. Cuautle,[62] L. Cunqueiro,[61] T. Dahms,[35,97] A. Dainese,[110] M. C. Danisch,[96] A. Danu,[58] D. Das,[103] I. Das,[103] S. Das,[4] A. Dash,[81] S. Dash,[47] S. De,[48,123] A. De Caro,[29] G. de Cataldo,[106] C. de Conti,[123] J. de Cuveland,[41] A. De Falco,[23] D. De Gruttola,[12,29] N. De Marco,[113] S. De Pasquale,[29] R. D. De Souza,[124] H. F. Degenhardt,[123] A. Deisting,[100,96] A. Deloff,[79] C. Deplano,[85] P. Dhankher,[47] D. Di Bari,[32] A. Di Mauro,[34] P. Di Nezza,[73] B. Di Ruzza,[110] M. A. Diaz Corchero,[10] T. Dietel,[92] P. Dillenseger,[60] R. Divià,[34] Ø. Djuvsland,[21] A. Dobrin,[58,34] D. Domenicis Gimenez,[123] B. Dönigus,[60] O. Dordic,[20] T. Drozhzhova,[60] A. K. Dubey,[139] A. Dubla,[100] L. Ducroux,[134] A. K. Duggal,[91] P. Dupieux,[71] R. J. Ehlers,[143] D. Elia,[106] E. Endress,[105] H. Engel,[59] E. Epple,[143] B. Erazmus,[116] F. Erhardt,[133] B. Espagnon,[51] S. Esumi,[132] G. Eulisse,[34] J. Eum,[99] D. Evans,[104] S. Evdokimov,[114] L. Fabbietti,[35,97] D. Fabris,[110] J. Faivre,[72] A. Fantoni,[73] M. Fasel,[88,75] L. Feldkamp,[61] A. Feliciello,[113] G. Feofilov,[138] J. Ferencei,[87] A. Fernández Téllez,[2] E. G. Ferreiro,[16] A. Ferretti,[25] A. Festanti,[28] V. J. G. Feuillard,[71,65] J. Figiel,[120] M. A. S. Figueredo,[123] S. Filchagin,[102] D. Finogeev,[52] F. M. Fionda,[23] E. M. Fiore,[32] M. Floris,[34] S. Foertsch,[66] P. Foka,[100] S. Fokin,[83] E. Fragiacomo,[112] A. Francescon,[34] A. Francisco,[116] U. Frankenfeld,[100] G. G. Fronze,[25] U. Fuchs,[34] C. Furget,[72] A. Furs,[52] M. Fusco Girard,[29] J. J. Gaardhøje,[84] M. Gagliardi,[25] A. M. Gago,[105] K. Gajdosova,[84] M. Gallio,[25] C. D. Galvan,[122] D. R. Gangadharan,[75] P. Ganoti,[78] C. Gao,[7] C. Garabatos,[100] E. Garcia-Solis,[13] K. Garg,[27] P. Garg,[48] C. Gargiulo,[34] P. Gasik,[35,97] E. F. Gauger,[121] M. B. Gay Ducati,[63] M. Germain,[116] P. Ghosh,[139] S. K. Ghosh,[4] P. Gianotti,[73] P. Giubellino,[34,113] P. Giubilato,[28] E. Gladysz-Dziadus,[120] P. Glässel,[96] D. M. Gómez Coral,[64] A. Gomez Ramirez,[59] A. S. Gonzalez,[34] V. Gonzalez,[10] P. González-Zamora,[10] S. Gorbunov,[41] L. Görlich,[120] S. Gotovac,[119] V. Grabski,[64] L. K. Graczykowski,[140] K. L. Graham,[104] J. L. Gramling,[96] L. Greiner,[75] A. Grelli,[53] C. Grigoras,[34] V. Grigoriev,[76] A. Grigoryan,[1] S. Grigoryan,[67] N. Grion,[112] J. M. Gronefeld,[100] F. Grosa,[30] J. F. Grosse-Oetringhaus,[34] R. Grosso,[100] L. Gruber,[115] F. R. Grull,[59] F. Guber,[52] R. Guernane,[34,72] B. Guerzoni,[26] K. Gulbrandsen,[84] T. Gunji,[131] A. Gupta,[93] R. Gupta,[93] I. B. Guzman,[2] R. Haake,[34,61] C. Hadjidakis,[51] H. Hamagaki,[77,131] G. Hamar,[142] J. C. Hamon,[135] J. W. Harris,[143] A. Harton,[13] D. Hatzifotiadou,[107] S. Hayashi,[131] S. T. Heckel,[60] E. Hellbär,[60] H. Helstrup,[36] A. Herghelegiu,[80] G. Herrera Corral,[11] F. Herrmann,[61] B. A. Hess,[95] K. F. Hetland,[36] H. Hillemanns,[34] B. Hippolyte,[135] J. Hladky,[56] D. Horak,[38] R. Hosokawa,[132] P. Hristov,[34] C. Hughes,[129] T. J. Humanic,[18] N. Hussain,[43] T. Hussain,[17] D. Hutter,[41] D. S. Hwang,[19] R. Ilkaev,[102] M. Inaba,[132] M. Ippolitov,[83,76] M. Irfan,[17] V. Isakov,[52] M. S. Islam,[48] M. Ivanov,[34,100] V. Ivanov,[89] V. Izucheev,[114] B. Jacak,[75] N. Jacazio,[26] P. M. Jacobs,[75] M. B. Jadhav,[47] S. Jadlovska,[118] J. Jadlovsky,[118] C. Jahnke,[35] M. J. Jakubowska,[140] M. A. Janik,[140] P. H. S. Y. Jayarathna,[126] C. Jena,[81] S. Jena,[126] M. Jercic,[133] R. T. Jimenez Bustamante,[100] P. G. Jones,[104] A. Jusko,[104] P. Kalinak,[55] A. Kalweit,[34] J. H. Kang,[144] V. Kaplin,[76] S. Kar,[139] A. Karasu Uysal,[70] O. Karavichev,[52] T. Karavicheva,[52] L. Karayan,[100,96] E. Karpechev,[52] U. Kebschull,[59] R. Keidel,[145] D. L. D. Keijdener,[53] M. Keil,[34] B. Ketzer,[44] M. Mohisin Khan,[17,§] P. Khan,[103] S. A. Khan,[139] A. Khanzadeev,[89] Y. Kharlov,[114] A. Khatun,[17] A. Khuntia,[48] M. M. Kielbowicz,[120] B. Kileng,[36] D. W. Kim,[42] D. J. Kim,[127] D. Kim,[144]

H. Kim,[144] J. S. Kim,[42] J. Kim,[96] M. Kim,[50] M. Kim,[144] S. Kim,[19] T. Kim,[144] S. Kirsch,[41] I. Kisel,[41] S. Kiselev,[54] A. Kisel,[140]
G. Kiss,[142] J. L. Klay,[6] C. Klein,[60] J. Klein,[34] C. Klein-Bösing,[61] S. Klewin,[96] A. Kluge,[34] M. L. Knichel,[96] A. G. Knospe,[126]
C. Kobdaj,[117] M. Kofarago,[34] T. Kollegger,[100] A. Kolojvari,[138] V. Kondratiev,[138] N. Kondratyeva,[76] E. Kondratyuk,[114]
A. Konevskikh,[52] M. Kopcik,[118] M. Kour,[93] C. Kouzinopoulos,[34] O. Kovalenko,[79] V. Kovalenko,[138] M. Kowalski,[120]
G. Koyithatta Meethaleveedu,[47] I. Králik,[55] A. Kravčáková,[39] M. Krivda,[55,104] F. Krizek,[87] E. Kryshen,[89] M. Krzewicki,[41]
A. M. Kubera,[18] V. Kučera,[87] C. Kuhn,[135] P. G. Kuijer,[85] A. Kumar,[93] J. Kumar,[47] L. Kumar,[91] S. Kumar,[47] S. Kundu,[81]
P. Kurashvili,[79] A. Kurepin,[52] A. B. Kurepin,[52] A. Kuryakin,[102] S. Kushpil,[87] M. J. Kweon,[50] Y. Kwon,[144] S. L. La Pointe,[41]
P. La Rocca,[27] C. Lagana Fernandes,[123] I. Lakomov,[34] R. Langoy,[40] K. Lapidus,[143] C. Lara,[59] A. Lardeux,[20,65] A. Lattuca,[25]
E. Laudi,[34] R. Lavicka,[38] L. Lazaridis,[34] R. Lea,[24] L. Leardini,[96] S. Lee,[144] F. Lehas,[85] S. Lehner,[115] J. Lehrbach,[41]
R. C. Lemmon,[86] V. Lenti,[106] E. Leogrande,[53] I. León Monzón,[122] P. Lévai,[142] S. Li,[7] X. Li,[14] J. Lien,[40] R. Lietava,[104]
S. Lindal,[20] V. Lindenstruth,[41] C. Lippmann,[100] M. A. Lisa,[18] V. Litichevskyi,[45] H. M. Ljunggren,[33] W. J. Llope,[141]
D. F. Lodato,[53] V. R. Loggins,[141] P. I. Loenne,[21] V. Loginov,[76] C. Loizides,[75] P. Loncar,[119] X. Lopez,[71] E. López Torres,[9]
A. Lowe,[142] P. Luettig,[60] M. Lunardon,[28] G. Luparello,[24] M. Lupi,[34] T. H. Lutz,[143] A. Maevskaya,[52] M. Mager,[34]
S. Mahajan,[93] S. M. Mahmood,[20] A. Maire,[135] R. D. Majka,[143] M. Malaev,[89] I. Maldonado Cervantes,[62] L. Malinina,[67,‖]
D. Mal'Kevich,[54] P. Malzacher,[100] A. Mamonov,[102] V. Manko,[83] F. Manso,[71] V. Manzari,[106] Y. Mao,[7] M. Marchisone,[66,130]
J. Mareš,[56] G. V. Margagliotti,[24] A. Margotti,[107] J. Margutti,[53] A. Marín,[100] C. Markert,[121] M. Marquard,[60] N. A. Martin,[100]
P. Martinengo,[34] J. A. L. Martinez,[59] M. I. Martínez,[2] G. Martínez García,[116] M. Martinez Pedreira,[34] A. Mas,[123]
S. Masciocchi,[100] M. Masera,[25] A. Masoni,[108] A. Mastroserio,[32] A. M. Mathis,[97,35] A. Matyja,[120,129] C. Mayer,[120]
J. Mazer,[129] M. Mazzilli,[32] M. A. Mazzoni,[111] F. Meddi,[22] Y. Melikyan,[76] A. Menchaca-Rocha,[64] E. Meninno,[29]
J. Mercado Pérez,[96] M. Meres,[37] S. Mhlanga,[92] Y. Miake,[132] M. M. Mieskolainen,[45] D. Mihaylov,[97] K. Mikhaylov,[67,54]
L. Milano,[75] J. Milosevic,[20] A. Mischke,[53] A. N. Mishra,[48] D. Miśkowiec,[100] J. Mitra,[139] C. M. Mitu,[58] N. Mohammadi,[53]
B. Mohanty,[81] E. Montes,[10] D. A. Moreira De Godoy,[61] L. A. P. Moreno,[2] S. Moretto,[28] A. Morreale,[116] A. Morsch,[34]
V. Muccifora,[73] E. Mudnic,[119] D. Mühlheim,[61] S. Muhuri,[139] M. Mukherjee,[139] J. D. Mulligan,[143] M. G. Munhoz,[123]
K. Münning,[44] R. H. Munzer,[35,97,60] H. Murakami,[131] S. Murray,[66] L. Musa,[34] J. Musinsky,[55] C. J. Myers,[126] B. Naik,[47]
R. Nair,[79] B. K. Nandi,[47] R. Nania,[107] E. Nappi,[106] M. U. Naru,[15] H. Natal da Luz,[123] C. Nattrass,[129] S. R. Navarro,[2]
K. Nayak,[81] R. Nayak,[47] T. K. Nayak,[139] S. Nazarenko,[102] A. Nedosekin,[54] R. A. Negrao De Oliveira,[34] L. Nellen,[62]
S. V. Nesbo,[36] F. Ng,[126] M. Nicassio,[100] M. Niculescu,[58] J. Niedziela,[34] B. S. Nielsen,[84] S. Nikolaev,[83] S. Nikulin,[83]
V. Nikulin,[89] F. Noferini,[107,12] P. Nomokonov,[67] G. Nooren,[53] J. C. C. Noris,[2] J. Norman,[128] A. Nyanin,[83] J. Nystrand,[21]
H. Oeschler,[96] S. Oh,[143] A. Ohlson,[96,34] T. Okubo,[46] L. Olah,[142] J. Oleniacz,[140] A. C. Oliveira Da Silva,[123] M. H. Oliver,[143]
J. Onderwaater,[100] C. Oppedisano,[113] R. Orava,[45] M. Oravec,[118] A. Ortiz Velasquez,[62] A. Oskarsson,[33] J. Otwinowski,[120]
K. Oyama,[77] M. Ozdemir,[60] Y. Pachmayer,[96] V. Pacik,[84] D. Pagano,[137] P. Pagano,[29] G. Paić,[62] S. K. Pal,[139] P. Palni,[7]
J. Pan,[141] A. K. Pandey,[47] S. Panebianco,[65] V. Papikyan,[1] G. S. Pappalardo,[109] P. Pareek,[48] J. Park,[50] W. J. Park,[100]
S. Parmar,[91] A. Passfeld,[61] S. P. Pathak,[126] V. Paticchio,[106] R. N. Patra,[139] B. Paul,[113] H. Pei,[7] T. Peitzmann,[53] X. Peng,[7]
L. G. Pereira,[63] H. Pereira Da Costa,[65] D. Peresunko,[83,76] E. Perez Lezama,[60] V. Peskov,[60] Y. Pestov,[5] V. Petráček,[38]
V. Petrov,[114] M. Petrovici,[80] C. Petta,[27] R. P. Pezzi,[63] S. Piano,[112] M. Pikna,[37] P. Pillot,[116] L. O. D. L. Pimentel,[84]
O. Pinazza,[107,34] L. Pinsky,[126] D. B. Piyarathna,[126] M. Płoskoń,[75] M. Planinic,[133] J. Pluta,[140] S. Pochybova,[142]
P. L. M. Podesta-Lerma,[122] M. G. Poghosyan,[88] B. Polichtchouk,[114] N. Poljak,[133] W. Poonsawat,[117] A. Pop,[80]
H. Poppenborg,[61] S. Porteboeuf-Houssais,[71] J. Porter,[75] J. Pospisil,[87] V. Pozdniakov,[67] S. K. Prasad,[4] R. Preghenella,[34,107]
F. Prino,[113] C. A. Pruneau,[141] I. Pshenichnov,[52] M. Puccio,[25] G. Puddu,[23] P. Pujahari,[141] V. Punin,[102] J. Putschke,[141]
H. Qvigstad,[20] A. Rachevski,[112] S. Raha,[4] S. Rajput,[93] J. Rak,[127] A. Rakotozafindrabe,[65] L. Ramello,[31] F. Rami,[135]
D. B. Rana,[126] R. Raniwala,[94] S. Raniwala,[94] S. S. Räsänen,[45] B. T. Rascanu,[60] D. Rathee,[91] V. Ratza,[44] I. Ravasenga,[30]
K. F. Read,[88,129] K. Redlich,[79] A. Rehman,[21] P. Reichelt,[60] F. Reidt,[34] X. Ren,[7] R. Renfordt,[60] A. R. Reolon,[73] A. Reshetin,[52]
K. Reygers,[96] V. Riabov,[89] R. A. Ricci,[74] T. Richert,[53,33] M. Richter,[20] P. Riedler,[34] W. Riegler,[34] F. Riggi,[27] C. Ristea,[58]
M. Rodríguez Cahuantzi,[2] K. Røed,[20] E. Rogochaya,[67] D. Rohr,[41] D. Röhrich,[21] P. S. Rokita,[140] F. Ronchetti,[34,73]
L. Ronflette,[116] P. Rosnet,[71] A. Rossi,[28] A. Rotondi,[136] F. Roukoutakis,[78] A. Roy,[48] C. Roy,[135] P. Roy,[103]
A. J. Rubio Montero,[10] R. Rui,[24] R. Russo,[25] A. Rustamov,[82] E. Ryabinkin,[83] Y. Ryabov,[89] A. Rybicki,[120] S. Saarinen,[45]
S. Sadhu,[139] S. Sadovsky,[114] K. Šafařík,[34] S. K. Saha,[139] B. Sahlmuller,[60] B. Sahoo,[47] P. Sahoo,[48] R. Sahoo,[48] S. Sahoo,[57]
P. K. Sahu,[57] J. Saini,[139] S. Sakai,[73,132] M. A. Saleh,[141] J. Salzwedel,[18] S. Sambyal,[93] V. Samsonov,[76,89] A. Sandoval,[64]
D. Sarkar,[139] N. Sarkar,[139] P. Sarma,[43] M. H. P. Sas,[53] E. Scapparone,[107] F. Scarlassara,[28] R. P. Scharenberg,[98] H. S. Scheid,[60]

C. Schiaua,[80] R. Schicker,[96] C. Schmidt,[100] H. R. Schmidt,[95] M. O. Schmidt,[96] M. Schmidt,[95] J. Schukraft,[34] Y. Schutz,[116,135,34] K. Schwarz,[100] K. Schweda,[100] G. Scioli,[26] E. Scomparin,[113] R. Scott,[129] M. Šefčík,[39] J. E. Seger,[90] Y. Sekiguchi,[131] D. Sekihata,[46] I. Selyuzhenkov,[76,100] K. Senosi,[66] S. Senyukov,[3,135,34] E. Serradilla,[64,10] P. Sett,[47] A. Sevcenco,[58] A. Shabanov,[52] A. Shabetai,[116] O. Shadura,[3] R. Shahoyan,[34] A. Shangaraev,[114] A. Sharma,[93] A. Sharma,[91] M. Sharma,[93] M. Sharma,[93] N. Sharma,[129,91] A. I. Sheikh,[139] K. Shigaki,[46] Q. Shou,[7] K. Shtejer,[25,9] Y. Sibiriak,[83] S. Siddhanta,[108] K. M. Sielewicz,[34] T. Siemiarczuk,[79] D. Silvermyr,[33] C. Silvestre,[72] G. Simatovic,[133] G. Simonetti,[34] R. Singaraju,[139] R. Singh,[81] V. Singhal,[139] T. Sinha,[103] B. Sitar,[37] M. Sitta,[31] T. B. Skaali,[20] M. Slupecki,[127] N. Smirnov,[143] R. J. M. Snellings,[53] T. W. Snellman,[127] J. Song,[99] M. Song,[144] F. Soramel,[28] S. Sorensen,[129] F. Sozzi,[100] E. Spiriti,[73] I. Sputowska,[120] B. K. Srivastava,[98] J. Stachel,[96] I. Stan,[58] P. Stankus,[88] E. Stenlund,[33] J. H. Stiller,[96] D. Stocco,[116] P. Strmen,[37] A. A. P. Suaide,[123] T. Sugitate,[46] C. Suire,[51] M. Suleymanov,[15] M. Suljic,[24] R. Sultanov,[54] M. Šumbera,[87] S. Sumowidagdo,[49] K. Suzuki,[115] S. Swain,[57] A. Szabo,[37] I. Szarka,[37] A. Szczepankiewicz,[140] M. Szymanski,[140] U. Tabassam,[15] J. Takahashi,[124] G. J. Tambave,[21] N. Tanaka,[132] M. Tarhini,[51] M. Tariq,[17] M. G. Tarzila,[80] A. Tauro,[34] G. Tejeda Muñoz,[2] A. Telesca,[34] K. Terasaki,[131] C. Terrevoli,[28] B. Teyssier,[134] D. Thakur,[48] S. Thakur,[139] D. Thomas,[121] R. Tieulent,[134] A. Tikhonov,[52] A. R. Timmins,[126] A. Toia,[60] S. Tripathy,[48] S. Trogolo,[25] G. Trombetta,[32] V. Trubnikov,[3] W. H. Trzaska,[127] B. A. Trzeciak,[53] T. Tsuji,[131] A. Tumkin,[102] R. Turrisi,[110] T. S. Tveter,[20] K. Ullaland,[21] E. N. Umaka,[126] A. Uras,[134] G. L. Usai,[23] A. Utrobicic,[133] M. Vala,[118,55] J. Van Der Maarel,[53] J. W. Van Hoorne,[34] M. van Leeuwen,[53] T. Vanat,[87] P. Vande Vyvre,[34] D. Varga,[142] A. Vargas,[2] M. Vargyas,[127] R. Varma,[47] M. Vasileiou,[78] A. Vasiliev,[83] A. Vauthier,[72] O. Vázquez Doce,[97,35] V. Vechernin,[138] A. M. Veen,[53] A. Velure,[21] E. Vercellin,[25] S. Vergara Limón,[2] R. Vernet,[8] R. Vértesi,[142] L. Vickovic,[119] S. Vigolo,[53] J. Viinikainen,[127] Z. Vilakazi,[130] O. Villalobos Baillie,[104] A. Villatoro Tello,[2] A. Vinogradov,[83] L. Vinogradov,[138] T. Virgili,[29] V. Vislavicius,[33] A. Vodopyanov,[67] M. A. Völkl,[96] K. Voloshin,[54] S. A. Voloshin,[141] G. Volpe,[32] B. von Haller,[34] I. Vorobyev,[97,35] D. Voscek,[118] D. Vranic,[34,100] J. Vrláková,[39] B. Wagner,[21] J. Wagner,[100] H. Wang,[53] M. Wang,[7] D. Watanabe,[132] Y. Watanabe,[131] M. Weber,[115] S. G. Weber,[100] D. F. Weiser,[96] J. P. Wessels,[61] U. Westerhoff,[61] A. M. Whitehead,[92] J. Wiechula,[60] J. Wikne,[20] G. Wilk,[79] J. Wilkinson,[96] G. A. Willems,[61] M. C. S. Williams,[107] B. Windelband,[96] W. E. Witt,[129] S. Yalcin,[70] P. Yang,[7] S. Yano,[46] Z. Yin,[7] H. Yokoyama,[132,72] I.-K. Yoo,[34,99] J. H. Yoon,[50] V. Yurchenko,[3] V. Zaccolo,[84,113] A. Zaman,[15] C. Zampolli,[34] H. J. C. Zanoli,[123] S. Zaporozhets,[67] N. Zardoshti,[104] A. Zarochentsev,[138] P. Závada,[56] N. Zaviyalov,[102] H. Zbroszczyk,[140] M. Zhalov,[89] H. Zhang,[21,7] X. Zhang,[7,75] Y. Zhang,[7] C. Zhang,[53] Z. Zhang,[7] C. Zhao,[20] N. Zhigareva,[54] D. Zhou,[7] Y. Zhou,[84] Z. Zhou,[21] H. Zhu,[21,7] J. Zhu,[7,116] X. Zhu,[7] A. Zichichi,[12,26] A. Zimmermann,[96] M. B. Zimmermann,[34,61] S. Zimmermann,[115] G. Zinovjev,[3] and J. Zmeskal[115]

(ALICE Collaboration)

[1]*A.I. Alikhanyan National Science Laboratory (Yerevan Physics Institute) Foundation, Yerevan, Armenia*
[2]*Benemérita Universidad Autónoma de Puebla, Puebla, Mexico*
[3]*Bogolyubov Institute for Theoretical Physics, Kiev, Ukraine*
[4]*Bose Institute, Department of Physics and Centre for Astroparticle Physics and Space Science (CAPSS), Kolkata, India*
[5]*Budker Institute for Nuclear Physics, Novosibirsk, Russia*
[6]*California Polytechnic State University, San Luis Obispo, California, USA*
[7]*Central China Normal University, Wuhan, China*
[8]*Centre de Calcul de l'IN2P3, Villeurbanne, Lyon, France*
[9]*Centro de Aplicaciones Tecnológicas y Desarrollo Nuclear (CEADEN), Havana, Cuba*
[10]*Centro de Investigaciones Energéticas Medioambientales y Tecnológicas (CIEMAT), Madrid, Spain*
[11]*Centro de Investigación y de Estudios Avanzados (CINVESTAV), Mexico City and Mérida, Mexico*
[12]*Centro Fermi - Museo Storico della Fisica e Centro Studi e Ricerche "Enrico Fermi", Rome, Italy*
[13]*Chicago State University, Chicago, Illinois, USA*
[14]*China Institute of Atomic Energy, Beijing, China*
[15]*COMSATS Institute of Information Technology (CIIT), Islamabad, Pakistan*
[16]*Departamento de Física de Partículas and IGFAE, Universidad de Santiago de Compostela, Santiago de Compostela, Spain*
[17]*Department of Physics, Aligarh Muslim University, Aligarh, India*
[18]*Department of Physics, Ohio State University, Columbus, Ohio, USA*
[19]*Department of Physics, Sejong University, Seoul, South Korea*
[20]*Department of Physics, University of Oslo, Oslo, Norway*

[21]Department of Physics and Technology, University of Bergen, Bergen, Norway

[22]Dipartimento di Fisica dell'Università 'La Sapienza' and Sezione INFN, Rome, Italy

[23]Dipartimento di Fisica dell'Università and Sezione INFN, Cagliari, Italy

[24]Dipartimento di Fisica dell'Università and Sezione INFN, Trieste, Italy

[25]Dipartimento di Fisica dell'Università and Sezione INFN, Turin, Italy

[26]Dipartimento di Fisica e Astronomia dell'Università and Sezione INFN, Bologna, Italy

[27]Dipartimento di Fisica e Astronomia dell'Università and Sezione INFN, Catania, Italy

[28]Dipartimento di Fisica e Astronomia dell'Università and Sezione INFN, Padova, Italy

[29]Dipartimento di Fisica 'E.R. Caianiello' dell'Università and Gruppo Collegato INFN, Salerno, Italy

[30]Dipartimento DISAT del Politecnico and Sezione INFN, Turin, Italy

[31]Dipartimento di Scienze e Innovazione Tecnologica dell'Università del Piemonte Orientale and INFN Sezione di Torino,
Alessandria, Italy

[32]Dipartimento Interateneo di Fisica 'M. Merlin' and Sezione INFN, Bari, Italy

[33]Division of Experimental High Energy Physics, University of Lund, Lund, Sweden

[34]European Organization for Nuclear Research (CERN), Geneva, Switzerland

[35]Excellence Cluster Universe, Technische Universität München, Munich, Germany

[36]Faculty of Engineering, Bergen University College, Bergen, Norway

[37]Faculty of Mathematics, Physics and Informatics, Comenius University, Bratislava, Slovakia

[38]Faculty of Nuclear Sciences and Physical Engineering, Czech Technical University in Prague, Prague, Czech Republic

[39]Faculty of Science, P.J. Šafárik University, Košice, Slovakia

[40]Faculty of Technology, Buskerud and Vestfold University College, Tonsberg, Norway

[41]Frankfurt Institute for Advanced Studies, Johann Wolfgang Goethe-Universität Frankfurt, Frankfurt, Germany

[42]Gangneung-Wonju National University, Gangneung, South Korea

[43]Gauhati University, Department of Physics, Guwahati, India

[44]Helmholtz-Institut für Strahlen- und Kernphysik, Rheinische Friedrich-Wilhelms-Universität Bonn, Bonn, Germany

[45]Helsinki Institute of Physics (HIP), Helsinki, Finland

[46]Hiroshima University, Hiroshima, Japan

[47]Indian Institute of Technology Bombay (IIT), Mumbai, India

[48]Indian Institute of Technology Indore, Indore, India

[49]Indonesian Institute of Sciences, Jakarta, Indonesia

[50]Inha University, Incheon, South Korea

[51]Institut de Physique Nucléaire d'Orsay (IPNO), Université Paris-Sud, CNRS-IN2P3, Orsay, France

[52]Institute for Nuclear Research, Academy of Sciences, Moscow, Russia

[53]Institute for Subatomic Physics of Utrecht University, Utrecht, Netherlands

[54]Institute for Theoretical and Experimental Physics, Moscow, Russia

[55]Institute of Experimental Physics, Slovak Academy of Sciences, Košice, Slovakia

[56]Institute of Physics, Academy of Sciences of the Czech Republic, Prague, Czech Republic

[57]Institute of Physics, Bhubaneswar, India

[58]Institute of Space Science (ISS), Bucharest, Romania

[59]Institut für Informatik, Johann Wolfgang Goethe-Universität Frankfurt, Frankfurt, Germany

[60]Institut für Kernphysik, Johann Wolfgang Goethe-Universität Frankfurt, Frankfurt, Germany

[61]Institut für Kernphysik, Westfälische Wilhelms-Universität Münster, Münster, Germany

[62]Instituto de Ciencias Nucleares, Universidad Nacional Autónoma de México, Mexico City, Mexico

[63]Instituto de Física, Universidade Federal do Rio Grande do Sul (UFRGS), Porto Alegre, Brazil

[64]Instituto de Física, Universidad Nacional Autónoma de México, Mexico City, Mexico

[65]IRFU, CEA, Université Paris-Saclay, F-91191 Gif-sur-Yvette, France, Saclay, France

[66]iThemba LABS, National Research Foundation, Somerset West, South Africa

[67]Joint Institute for Nuclear Research (JINR), Dubna, Russia

[68]Konkuk University, Seoul, South Korea

[69]Korea Institute of Science and Technology Information, Daejeon, South Korea

[70]KTO Karatay University, Konya, Turkey

[71]Laboratoire de Physique Corpusculaire (LPC), Clermont Université, Université Blaise Pascal,
CNRS–IN2P3, Clermont-Ferrand, France

[72]Laboratoire de Physique Subatomique et de Cosmologie, Université Grenoble-Alpes, CNRS-IN2P3, Grenoble, France

[73]Laboratori Nazionali di Frascati, INFN, Frascati, Italy

[74]Laboratori Nazionali di Legnaro, INFN, Legnaro, Italy

[75]Lawrence Berkeley National Laboratory, Berkeley, California, USA

[76]Moscow Engineering Physics Institute, Moscow, Russia

[77]Nagasaki Institute of Applied Science, Nagasaki, Japan

[78]National and Kapodistrian University of Athens, Physics Department, Athens, Greece, Athens, Greece

[79]National Centre for Nuclear Studies, Warsaw, Poland

[80]National Institute for Physics and Nuclear Engineering, Bucharest, Romania

[81]National Institute of Science Education and Research, Bhubaneswar, India

[82]National Nuclear Research Center, Baku, Azerbaijan

[83]National Research Centre Kurchatov Institute, Moscow, Russia

[84]Niels Bohr Institute, University of Copenhagen, Copenhagen, Denmark

[85]Nikhef, Nationaal instituut voor subatomaire fysica, Amsterdam, Netherlands

[86]Nuclear Physics Group, STFC Daresbury Laboratory, Daresbury, United Kingdom

[87]Nuclear Physics Institute, Academy of Sciences of the Czech Republic, Řež u Prahy, Czech Republic

[88]Oak Ridge National Laboratory, Oak Ridge, Tennessee, USA

[89]Petersburg Nuclear Physics Institute, Gatchina, Russia

[90]Physics Department, Creighton University, Omaha, Nebraska, USA

[91]Physics Department, Panjab University, Chandigarh, India

[92]Physics Department, University of Cape Town, Cape Town, South Africa

[93]Physics Department, University of Jammu, Jammu, India

[94]Physics Department, University of Rajasthan, Jaipur, India

[95]Physikalisches Institut, Eberhard Karls Universität Tübingen, Tübingen, Germany

[96]Physikalisches Institut, Ruprecht-Karls-Universität Heidelberg, Heidelberg, Germany

[97]Physik Department, Technische Universität München, Munich, Germany

[98]Purdue University, West Lafayette, Indiana, USA

[99]Pusan National University, Pusan, South Korea

[100]Research Division and ExtreMe Matter Institute EMMI, GSI Helmholtzzentrum für Schwerionenforschung GmbH,
Darmstadt, Germany

[101]Rudjer Bošković Institute, Zagreb, Croatia

[102]Russian Federal Nuclear Center (VNIIEF), Sarov, Russia

[103]Saha Institute of Nuclear Physics, Kolkata, India

[104]School of Physics and Astronomy, University of Birmingham, Birmingham, United Kingdom

[105]Sección Física, Departamento de Ciencias, Pontificia Universidad Católica del Perú, Lima, Peru

[106]Sezione INFN, Bari, Italy

[107]Sezione INFN, Bologna, Italy

[108]Sezione INFN, Cagliari, Italy

[109]Sezione INFN, Catania, Italy

[110]Sezione INFN, Padova, Italy

[111]Sezione INFN, Rome, Italy

[112]Sezione INFN, Trieste, Italy

[113]Sezione INFN, Turin, Italy

[114]SSC IHEP of NRC Kurchatov institute, Protvino, Russia

[115]Stefan Meyer Institut für Subatomare Physik (SMI), Vienna, Austria

[116]SUBATECH, Ecole des Mines de Nantes, Université de Nantes, CNRS-IN2P3, Nantes, France

[117]Suranaree University of Technology, Nakhon Ratchasima, Thailand

[118]Technical University of Košice, Košice, Slovakia

[119]Technical University of Split FESB, Split, Croatia

[120]The Henryk Niewodniczanski Institute of Nuclear Physics, Polish Academy of Sciences, Cracow, Poland

[121]The University of Texas at Austin, Physics Department, Austin, Texas, USA

[122]Universidad Autónoma de Sinaloa, Culiacán, Mexico

[123]Universidade de S ao Paulo (USP), S ao Paulo, Brazil

[124]Universidade Estadual de Campinas (UNICAMP), Campinas, Brazil

[125]Universidade Federal do ABC, Santo Andre, Brazil

[126]University of Houston, Houston, Texas, USA

[127]University of Jyväskylä, Jyväskylä, Finland

[128]University of Liverpool, Liverpool, United Kingdom

[129]University of Tennessee, Knoxville, Tennessee, USA

[130]University of the Witwatersrand, Johannesburg, South Africa

[131]University of Tokyo, Tokyo, Japan

[132]University of Tsukuba, Tsukuba, Japan

[133]University of Zagreb, Zagreb, Croatia

[134]Université de Lyon, Université Lyon 1, CNRS/IN2P3, IPN-Lyon, Villeurbanne, Lyon, France

[135]Université de Strasbourg, CNRS, IPHC UMR 7178, F-67000 Strasbourg, France, Strasbourg, France

[136]Università degli Studi di Pavia, Pavia, Italy

[137]Università di Brescia, Brescia, Italy

[138]*V. Fock Institute for Physics, St. Petersburg State University, St. Petersburg, Russia*
[139]*Variable Energy Cyclotron Centre, Kolkata, India*
[140]*Warsaw University of Technology, Warsaw, Poland*
[141]*Wayne State University, Detroit, Michigan, USA*
[142]*Wigner Research Centre for Physics, Hungarian Academy of Sciences, Budapest, Hungary*
[143]*Yale University, New Haven, Connecticut, USA*
[144]*Yonsei University, Seoul, South Korea*
[145]*Zentrum für Technologietransfer und Telekommunikation (ZTT), Fachhochschule Worms, Worms, Germany*

[†]Deceased.
[‡]Also at Georgia State University, Atlanta, Georgia, USA.
[§]Also at Department of Applied Physics, Aligarh Muslim University, Aligarh, India.
[‖]Also at M.V. Lomonosov Moscow State University, D.V. Skobeltsyn Institute of Nuclear, Physics, Moscow, Russia.